ARTICLE IN PRESS

Journal of Pharmaceutical Sciences 000 (2024) 1-7

FISEVIER

Contents lists available at ScienceDirect

Journal of Pharmaceutical Sciences

journal homepage: www.jpharmsci.org



Pharmaceutics, Drug Delivery and Pharmaceutical Technology

Crystallization Inhibition in Molecular Liquids by Polymers above the Overlap Concentration (c^*): Delay of the First Nucleation Event

Sichen Song^{a,b}, Shuquan Cui^c, Changquan Calvin Sun^a, Timothy P. Lodge^{c,d}, Ronald A. Siegel^{a,e,*}

- ^a Department of Pharmaceutics, University of Minnesota, Minneapolis, MN 55455, United States
- ^b School of Mathematics, University of Minnesota, Minneapolis, MN 55455, United States
- ^c Department of Chemistry, University of Minnesota, Minneapolis, MN 55455, United States
- ^d Department of Chemical Engineering and Materials Science, University of Minnesota, Minneapolis, MN 55455, United States
- ^e Department of Biomedical Engineering, University of Minnesota, Minneapolis, MN 55455, United States

ARTICLE INFO

Article history: Received 12 January 2024 Revised 9 February 2024 Accepted 9 February 2024 Available online xxx

Keywords:
Amorphous solid dispersion (ASD)
Physical stability
Crystal nucleation
Crystal growth
Polymer overlap concentration (c*)

ABSTRACT

Low concentration polymer additives can significantly alter crystal growth kinetics of molecular liquids and glasses. However, the effect of polymer concentration on nucleation kinetics remains poorly understood. Based on an experimentally determined first nucleation time (time to form the first critical nucleus, t_0), we show that the polymer overlap concentration, c^* , where polymer coils in the molecular liquid start to overlap with each other, is a critical polymer concentration for efficient inhibition of crystallization of a molecular liquid. The value of t_0 is approximately equal to that of the neat molecular liquid when the polymer concentration, c, is below c^* , but increases significantly when $c > c^*$. This finding is relevant for effective polymer screening and performance prediction of engineered multicomponent amorphous materials, particularly pharmaceutical amorphous solid dispersions.

© 2024 American Pharmacists Association. Published by Elsevier Inc. All rights reserved.

Introduction

Glasses are amorphous solids that can be formed by several processes, such as melt quenching, solvent evaporation, and vapor deposition, while preventing crystallization. Glasses exhibit both the spatial uniformity of liquids and the mechanical strength of solids, making them useful in manufacturing a wide range of materials, such as windows, hard plastic products, and dense granular assemblies. In the pharmaceutical realm, the relatively high energy glassy state is commonly used to enhance oral bioavailability of drugs whose lower energy crystalline forms are poorly soluble in aqueous media. Successful application of glassy materials requires inhibition against crystallization.

Crystallization occurs by two steps, nucleation and growth, with both exhibiting distinct kinetics.⁶ Because of their strong inhibitory effect on both nucleation and growth processes of molecular glasses,⁷ polymers are commonly incorporated to engineer multicomponent amorphous materials, such as pharmaceutical amorphous solid

E-mail address: siege017@umn.edu (R.A. Siegel).

dispersions and functional biomaterials for regenerative medicine appilcations. A central question in designing multicomponent organic glasses is "what is the minimum polymer concentration for effective inhibition of crystallization?" Multicomponent amorphous materials with a minimal polymer concentration while maintaining stability, have advantages. For example, pharmaceutical amorphous formulations with a lower polymer content improve patient compliance by reducing pill burden (tablet size and dosage units), as well as simplifying downstream processing in large scale manufacturing. 10

Using polyvinylpyrrolidones (PVPs) with different molecular weights, ranging from 4 to 120 kDa, and four different molecular glasses, namely celecoxib (CEL), loratadine, indomethacin, and felodipine, we recently showed that the lowest polymer concentration capable of effectively reducing crystallization of molecular glasses can be estimated by the overlap concentration, c^* , where polymer coils start to contact each other in the composite glass. ^{11,12} For example, the crystallization tendency of CEL in an amorphous dispersion is identical to that of pure amorphous CEL when the PVP concentration is lower than c^* , but enhanced physical stability of CEL is observed when PVP concentration exceeds $c^{*,11}$ Experimental results with other common pharmaceutical drugs and polymers have confirmed that c^* approximates the minimal polymer concentration required to

^{*} Corresponding author at: Department of Pharmaceutics, University of Minnesota, Minneapolis, MN 55455, United States.

inhibit drug crystallization. ¹³ Despite the apparent universality of this phenomenon, the precise mechanism of the crystallization inhibition effect of polymers above c^* remains unknown.

Research over the past two decades has focused on the effect of low concentration (<10 %, w/w) polymer additives on steady state rates of nucleation and growth of crystals in molecular glasses and liquids. $^{7,14-17}$ However, the first nucleation time, t_0 , defined as the time to form the first group of critical nuclei in a fresh amorphous material, is also of importance in describing homogenous nucleation kinetics. $^{18-20}$ A material is no longer purely amorphous beyond t_0 , which marks the onset of likely catastrophic performance degradation. For example, pharmaceutical amorphous formulations containing residual crystal nuclei lose their dissolution and oral bioavailability advantage compared with the nucleus-free form. $^{21-23}$ Despite its practical importance, there has been no experimental study of t_0 in glass forming molecular systems.

In the present study, we systematically investigate the effect of concentration, c, of a model polymer polyvinylpyrrolidone (PVP, four molecular weights) on t_0 and the steady state rates of crystal nucleation and growth of a model molecular liquid, D-sorbitol, which has been widely used in the pharmaceutical, food, and textile industries. We show that t_0 of molecular liquid/polymer combinations is approximately identical to that of the neat liquid when $c < c^*$, but is significantly larger when $c > c^*$. We also show, however, that rates of nucleation and growth decrease exponentially over the entire concentration range with no abrupt change at c^* . Thus, the inhibitory effect against crystallization by a polymer above its c^* is primarily correlated with the delay in the first nucleation event. Our findings are relevant for the efficient design of multicomponent amorphous materials with sufficient physical stability by identifying optimal polymer type and concentration.

Materials and Methods

Materials

D-sorbitol (γ polymorph with purity \geq 99 %, see Fig. S1) was purchased from Huakang Pharmaceutical. Polyvinylpyrrolidones (PVPs; K12, K17, K25, and K30) were obtained from BASF. Ethanol was purchased from VWR. D-sorbitol was used both as received and after recrystallization. Recrystallization was performed as follows: D-sorbitol was dissolved in ethanol at \sim 110 °C and the hot solution was immediately filtered by passing through a 0.22 μ m syringe filter. The resultant solution was cooled at room temperature for 24 h. After complete crystallization, the mother liquor was decanted, and the crystals were washed twice with ethanol and completely dried under vacuum. PVPs were used as received. Table 1 shows the molecular structures of D-sorbitol and PVPs and their relevant physical properties.

Sample Preparation

D-sorbitol/PVP uniform physical mixtures were prepared by cryogenic milling with a Spex SamplePrep Grinder 6770 (liquid N_2 as coolant). Cryomilling was performed at 10 Hz for five 2 min cycles, each followed by a 2 min cool down. D-sorbitol/PVP powder mixture was placed on a glass slide and melted at 150 °C for \sim 1 h to remove air bubbles. A coverslip was then placed on the melt to produce a sandwiched film with 15–20 μ m thickness. The sandwiched liquid film was quenched to 34 °C by contacting a preheated metal block.

Viscometry

Zero-shear-rate viscosity (η) of pure D-sorbitol and D-sorbitol/PVP melts was measured at 155 °C using an ARES rheometer. A parallel plate geometry with diameter 25 mm was employed. Briefly, approximately 700 mg of powder was placed on the bottom plate after zero torque, normal force, and gap calibrations. The gap between the parallel plates was approximately 1 mm. A steady rate sweep test was performed with initial rate of 1 s⁻¹ and final rate of 100 s⁻¹ with continuous N₂ purge at a flow rate of 3 standard cubic feet per minute.

Crystal Growth Rates

Crystal growth rates of D-sorbitol without or with PVP at 34 °C were measured using an Olympus BX51 polarized light microscope equipped with a Linkam LTS420 thermal stage (thermal stability \leq 0.1 °C with continuous dry N_2 purge) by tracking the advance of spherulite growth fronts over time. Each reported rate was an average of 13–25 measurements of three separate samples. All growth rates were found to be constant over time.

Nucleation Rates

Freshly prepared sandwiched samples were stored in desiccators [0 % relative humidity (RH)] at 34 °C maintained within a heating chamber (temperature stability \leq 0.4 °C) for an arbitrary observation time t, at which point the radius of individual spherulites, r, was measurable. The birth time of each spherulite t_n was calculated as $t_n = t - r/u$, where u is the crystal growth rate. Tracking the birth time of individual crystals enabled the determination of nuclei density over time. The nucleation rate was extrapolated from the nuclei density-time plot at steady state. Each reported rate was an average of 3–4 measurements of three separate samples.

First Nucleation Times

Determination of the first nucleation time of freshly prepared sandwiched samples at 34 $^{\circ}\text{C}$ and 0 % RH is described in Results and Discussion.

Table 1Molecular structures and relevant physical properties of D-sorbitol and PVP.

	Molecular structure	$M_{\rm w}({\rm g/mol})^*$	$\mathcal{D}\left(M_{\rm w}/M_{\rm n}\right)^*$	$T_{\rm g}(^{\circ}{ m C})$	T_{m} (°C)
D-sorbitol	HO OH OH	182.2	-	0.82	95.20
PVP K12 PVP K17 PVP K25 PVP K30	N = 0	3800 7300 49,500 55,000	1.65 1.81 1.92 1.81	102 138 165 171	- - - -

^{*} $M_{\rm w}$ and D of PVPs were determined in the previous work. 11

Small Angle X-ray Scattering (SAXS)

Synchrotron SAXS experiments were performed at the Sector 5-ID-D beamline (λ = 0.7293 Å) at the Advanced Photon Source, Argonne National Laboratory. Samples were sealed in Tzero aluminum pans under argon. SAXS data was collected on a Rayonix MX 170-HS detector with an 8.5 m sample-to-detector distance, giving a range for the scattering vector magnitude q of $2.5 \times 10^{-3} - 0.195$ Å. Center and size of azimuth range were 315° and 120°, respectively. The exposure time was 1 s for each measurement.

Solid State Characterization

Differential scanning calorimetry (DSC) was performed with a TA Q1000 in a Tzero aluminum pan with a pinhole under continuous helium purge at a flow rate of 25 mL/min. Samples (5–10 mg) were first heated from 40 °C to 120 °C at 10 °C/min to erase thermal history, quenched to -30 °C, held isothermally for 3 min, and reheated at 10 °C/min to 120 °C. Melting point depression of D-sorbitol by PVP was evaluated during the first heating cycle, while glass transition temperatures, $T_{\rm g}$, were measured during the second heating cycle. The D-sorbitol crystal polymorph was identified using an X'pert Pro X-ray diffractometer with a Cu K α source λ = 1.540598 Å. Powder samples were scanned over the range 2θ = 5–35° with step size 0.016° at 1 s/step. Tube voltage and amperage were set as 45 kV and 40 mA, respectively.

Results and Discussion

The Overlap Concentration, c^* , of PVPs in D-sorbitol

Values of c^* for various PVPs dissolved in D-sorbitol at 155 °C were estimated from (zero shear) viscosity-composition curves by locating the transition between the linear and nonlinear regimes (Fig. 1). In a good solvent, polymer coils in the dilute regime are isolated from each other (Fig. 2b), and intermolecular interactions between adjacent coils are negligible. Hence, the overall viscosity, η , is a linear function of polymer concentration, c (in wt%), following $\eta = \eta_s (1 + c[\eta]_w)$, where η_s is the viscosity of the neat molecular liquid, and $[\eta]_w$ is the intrinsic viscosity of molecular liquid/polymer (in wt% $^{-1}$). I1,25 The trend in η becomes nonlinear when polymer coils

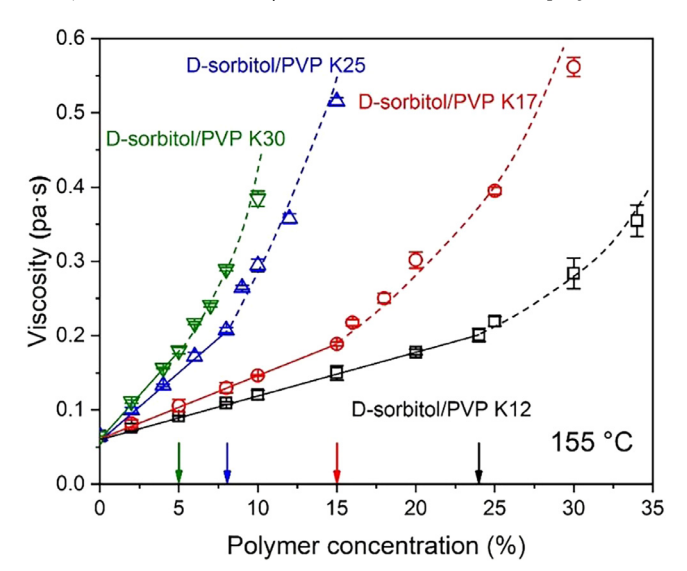


Fig. 1. Viscosity-composition diagram of D-sorbitol/PVP melts at 155 °C. Arrows correspond to c^* in the four systems, where there is a break in the slopes of the individual viscosity-polymer concentration curves ($n \ge 4$).

overlap, i.e., when intermolecular interactions between polymer coils become significant, in the semidilute regime (Fig. 2c, d). The crossover between the linear and nonlinear (dilute and semidilute) regimes happens at the overlap concentration, c^* , illustrated in Fig. 2c, which is delineated by arrows in Fig. 1. In the concentrated regime, viscosity increases more rapidly, partially due to polymer chain entanglement and slower polymer segmental mobility corresponding to a higher glass transition temperature (Fig. 2d). 25,26

D-sorbitol is a good solvent for PVP as confirmed by its progressive liquidus temperature depression with increasing PVP concentration (Fig. S2). The dependence of crystal growth rate, u, of D-sorbitol on polymer concentration also enables us to evaluate the state of mixing between D-sorbitol and PVPs. 14 For a compatible binary mixture, the crystal growth rate decreases exponentially with increasing polymer concentration, i.e., the log(u) vs. c curve is linear at constant temperature. A plateau would be found in a log(u) vs. c curve if phase separation occurred, e.g., nifedipine/polystyrene 17 K and 97 K. 14 All model systems studied in this work exhibit linear log(u) vs. c curves (see Figs. 5 and S3-S5). These two pieces of evidence confirm homogeneity of the systems during c^* measurement. 11,26 From the viscosity-composition plots of all D-sorbitol/PVP melts, measured at 155 °C to ensure complete melting, c* values for D-sorbitol/PVPs are approximately 24 % for PVP K12 (weight average molecular weight, $M_{\rm w} \approx 4$ K), 15 % for K17 ($M_{\rm w} \approx 8$ K), 8 % for K25 ($M_{\rm w} \approx 50$ K), and 5 % for K30 ($M_{\rm w} \approx 55$ K). Notice that the transition from the dilute to the semidilute regime is over a narrow range of polymer concentrations. With increasing M_w , c^* value decreases, in agreement with the polymer solution theory, which predicts that $c^* \sim M_{\rm w}^{-0.8}$. This relation reflects the fact that an isolated polymer chain with a higher $M_{\rm w}$ pervades a larger volume, which means a smaller c^* value for polymer coils to fill in the entire space.²⁶

The First Nucleation Time of D-sorbitol/PVPs

We previously showed that an effective inhibitory effect against crystallization of molecular liquids by polymer only occurs when $c > c^*, ^{11}$ but the mechanism for this observation was not elucidated. Here, we hypothesize that when $c < c^*$ (in the dilute regime), the gap between isolated polymer coils is sufficiently large that formation of critical nuclei of the molecular liquid cannot be delayed. If so, the first nucleation time, t_0 , will not be affected significantly by the presence of polymer (Fig. 2b). However, when $c > c^*$, the first nucleation event will be significantly delayed due to the absence of the pure liquid (amorphous drug) domain with sufficiently large volume (Fig. 2d).

We tested this hypothesis by determining t_0 in freshly prepared D-sorbitol/PVP liquids below and above c^* at 34 °C. Spontaneous homogeneous nucleation of D-sorbitol without and with PVP at 34 °C yields the polymorph E^{27} (Fig. S6); no other polymorphs $(\alpha,^{28} \gamma,^{29} \delta,$ and $\varepsilon^{30})$ were observed because of their extremely slow growth. The first nucleation time (t_0) of the system corresponds to the birth of the largest crystal observed in the entire sample, and is calculated from its current radius r, using $t_0 = t - r/u$, where t is the current time and u is the constant crystal growth rate under isothermal conditions, as illustrated in Fig. 3a. $^{6.7,18}$ As an example, shown in Fig. 3a, the t_0 of 10,600 s was observed for 2 % PVP K30/D-sorbitol held at 34 °C (the radius of the largest spherulite in the entire sample at $t = 7.86 \times 10^4$ s was 193 μ m and the growth rate was 2.84 nm/s).

Figure 3b shows values of t_0 for D-sorbitol as a function of polymer concentration c, rescaled by c^* for all four grades of PVP. In the PVP K25 and K30 (with higher $M_{\rm w}$) systems, the t_0 values are approximately identical to t_0 for neat D-sorbitol when $c \le c^*$, but increase gradually when $c > c^*$, as visualized by blue and green symbols and curves in Fig. 3b. These observations support our hypothesis. However, for the lower molecular weight polymers PVP K12 ($M_{\rm w} \approx 4$ K) and K17 ($M_{\rm w} \approx 8$ K), t_0 of D-sorbitol begins to increase at a

S. Song et al. / Journal of Pharmaceutical Sciences 00 (2024) 1-7

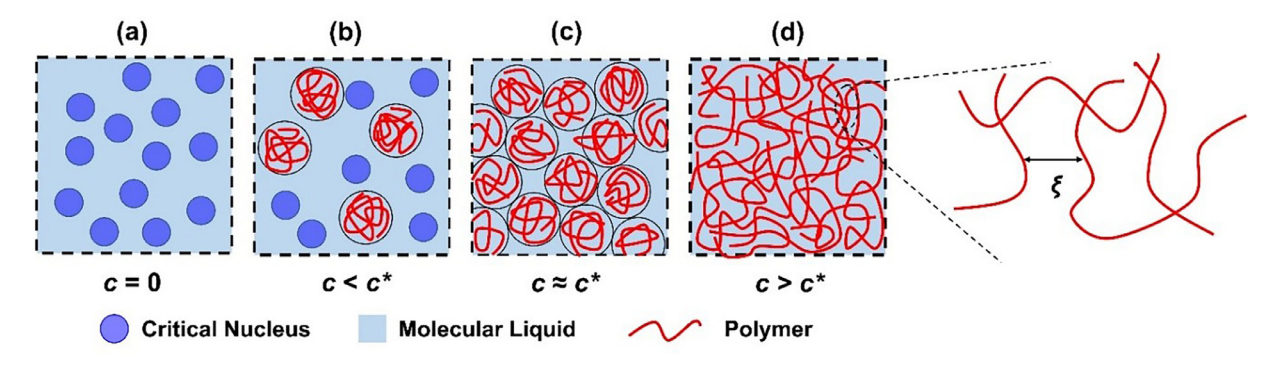


Fig. 2. Illustration of the delay of the first nucleation event in semi-dilute/concentrated (c, d) polymer solutions and schematics of correlation length ξ ($c^* < c \ll 1$) in (d). Light blue background indicates a molecular liquid serving as a solvent, red coils indicate polymers dissolved in the molecular liquid, and blue circles indicate critical nuclei of the glass forming molecular liquid.

concentration lower than c^* (0.625 c^* for PVP K12 and 0.667 c^* for PVP K17), shown by black and red symbols and curves, respectively, in Fig. 3b.

The effect of polymer molecular weight on t_0 can be explained by assuming that nucleation can commence without delay only when the critical nucleation radius, r_c , is less than the gap between adjacent polymer coils. According to polymer solution theory, an isolated polymer coil dissolved in a good solvent has radius of gyration $R_{\rm g} \sim M_{\rm w}^{0.6}$ and pervades a volume $\sim M_{\rm w}^{1.8}$. This indicates that polymer chains with greater $M_{\rm w}$ can occupy a larger space. Fig. 4a illustrates that when polymer $M_{\rm w}$ is relatively high, the $R_{\rm g}$ of a coil is much larger than the critical nucleus radius r_c . Therefore, the gap between coils is still large enough for the formation of critical nuclei

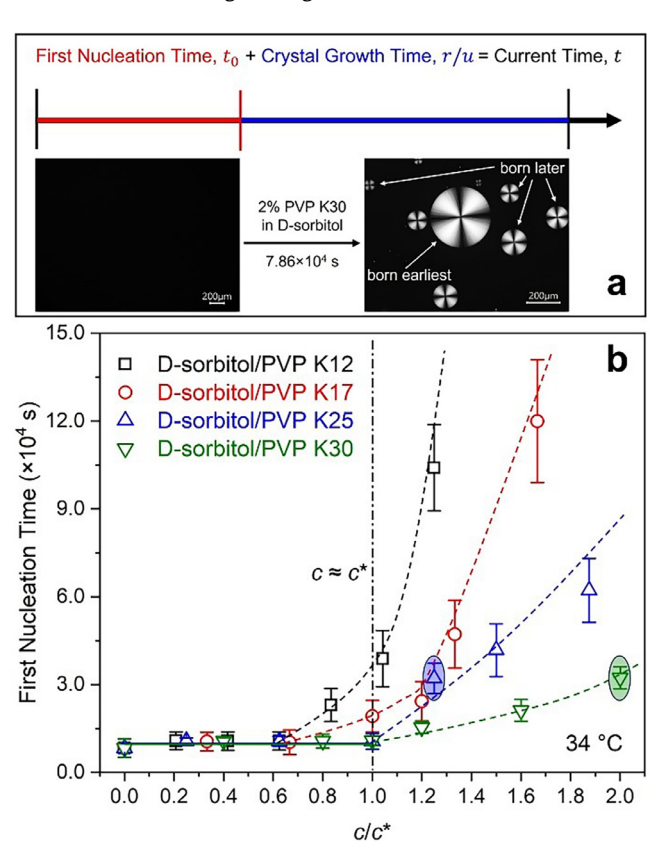


Fig. 3. (a) Scheme of the first nucleation time determination with an example of 2 % PVP K30 dissolved in D-sorbitol. (b) The first nucleation time of D-sorbitol/PVPs as a function of PVP concentration rescaled by c^* at 34 °C. Dashed curves are drawn to follow trends of increased first nucleation times with increasing polymer concentration (n = 28-299).

of the molecular liquid when $c \approx c^*$. A significant delay of the first nucleation event happens only when $c > c^*$. On the other hand, for relatively small polymers, $R_{\rm g}$ is comparable with r_c . Therefore, the gaps between adjacent coils even when c is slightly lower than c^* are sufficiently small for significantly delaying the first nucleation event

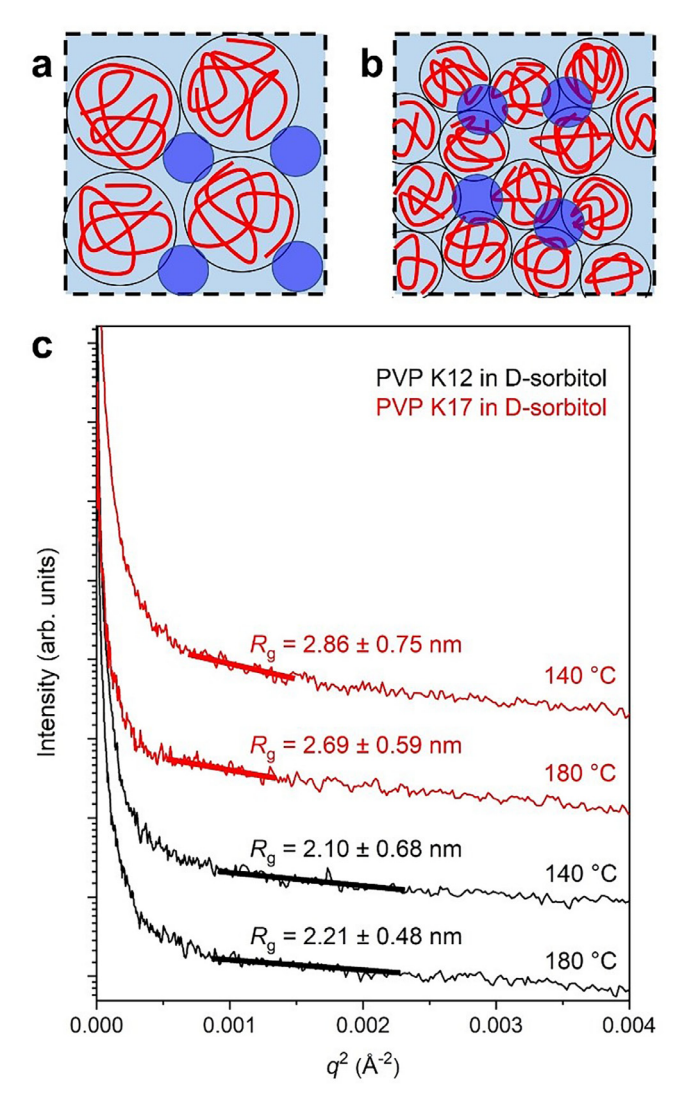


Fig. 4. Scheme of relative sizes of the polymer coil with (a) relatively large $M_{\rm w}$ and (b) small $M_{\rm w}$ and the critical nucleus when $c \approx c^*$. (c) Intensity of X-ray scattering of PVP K12 (black) and PVP K17 (red) dissolved in D-sorbitol as a function of q^2 at 140 °C and 180 °C.

S. Song et al. / Journal of Pharmaceutical Sciences 00 (2024) 1-7

(Fig. 4b). To better visualize this, consider peas and grapefruits. When grapefruits are packed together, there is room in the gaps for peas to be added. However, packed peas will not have room between them for other peas.

To support this hypothesis, we determined values of R_g of PVPs by X-ray scattering and compared these values with the radius of critical nuclei of D-sorbitol. It is assumed that r_c of D-sorbitol does not change in the presence of PVP. 32 Fig. 4c shows Guinier plots of scattering intensity $I_{\rm ex}$ for PVP K12 and K17 in D-sorbitol at 140 °C and 180 °C (c^* was measured at 155 °C, but c* in a good solvent does not change significantly with temperature 33). From these plots, the $R_{\rm g}$ s of PVP K12 and K17 were obtained by linear fitting in the Guinier regime, i.e., $qR_g \lesssim 1$, where *q* is the momentum transfer vector. In this regime, the form factor P(q) is given by $P(q) \approx \exp(-q^2 R_{\rm g}^2/3)$, and values of $R_{\rm g}$ can be obtained from linear portion of plots of $ln(I_{ex})$ versus q^2 with slope $-R_{\rm g}^2/3$, without any knowledge about the shape of the molecule.³¹ The determined R_g values of PVP K12 (approximately 2.1 nm) and PVP K17 (approximately 2.8 nm) are close to the radius of the critical nucleus r_c of D-sorbitol (approximately 1 nm at 34 °C) which is estimated by the classical nucleation theory to be $r_{\rm c}=2\sigma/\Delta G_{\rm V}$, where σ (0.013 J/m² for D-sorbitol) is the interfacial energy between crystal nucleus and liquid and ΔG_V ($\sim 2.7 \times 10^7$ J/m³ for D-sorbitol at 34 °C) is the bulk crystal/liquid free energy difference.⁶ Thus, delay of the first nucleation event occurs when the concentrations of PVP K12 and K17 are smaller than the corresponding c^* .

For PVP K25 and K30 with relatively higher molecular weight, a scaling analysis according to $R_{\rm g} \sim M_{\rm w}^{0.6}$ indicates that their $R_{\rm g}$ values (6.4 nm for PVP K25 and 6.7 nm for PVP K30) are approximately seven-fold larger than the radius of the critical nucleus of D-sorbitol. Since this size difference is significant, gaps between coils at c^* are large enough for the first nucleation event to occur unhindered (Fig. 4a). Consequently, a delay in the first nucleation event is observed only when c is greater than c^* .

Another intriguing observation from Fig. 3b is that the delay of formation of critical nuclei of D-sorbitol at $c > c^*$ do not follow a "master curve" with respect to c/c^* . This phenomenon must have been caused by the different $M_{\rm w}$ of PVPs since this is the only difference in this study. Here, we provide a tentative explanation of this observation with the assistance of Fig. 2c, d and a scaling analysis using polymer solution theory. In the semidilute regime (where polymer concentration, c, is slightly larger than c^*), the correlation length, ξ , (defined as the average mesh size between adjacent polymer chains, see Fig. 2d) in the scaling form versus the rescaled polymer concentration c/c^* can be constructed based on two facts: (1) when $c>c^*$, the scale of ξ depends on the polymer concentration alone, instead of $M_{\rm w}$, since ξ is smaller than the average chain length (Fig. 2d); (2) when $c \approx c^*$, coils start to overlap but are not yet entangled with neighboring chains, and ξ is comparable with the radius of an isolated coil $R_{\rm g}$ (Fig. 2c). These two facts lead to the scaling form: $\xi(c) \sim R_{\rm g}(c/c^*)^m$. The exponent m must be such that $R_{\rm g} \sim M_{\rm w}^{0.6}$ and $c^* \sim M_{\rm w}^{-0.8}$. Therefore, m = -0.75, i.e., $\xi(c) \sim c^{-0.75}$. This scaling relation reveals that $\boldsymbol{\xi}$ is a decreasing function of polymer concentration, c, provided $c > c^*$. Since ξ represents the spatial density of a polymer, a smaller ξ leads to a tighter mesh with less room for nuclei to form. Therefore, there is a more significant delay of the first nucleation event. The above scaling analysis suggests that the trend of the increasing t_0 versus c/c^* does not overlap when $c/c^* > 1$, which is consistent with the experimental results (Fig. 3b, blue and green dashed curves). Additionally, since ξ is a function of c in the semidilute regime, systems with same c are expected to exhibit comparable t_0 values. This is also consistent with our observations. For example, at the same polymer concentration of 10 % (wt/wt), which exceeds c* for both polymer molecular weights (in the semidilute regime), the value of t_0 in the PVP K25 system (32,000 \pm 5000 s) and the PVP K30 system $(32,000 \pm 4000 \text{ s})$ are comparable (Fig. 3b, oval circles).

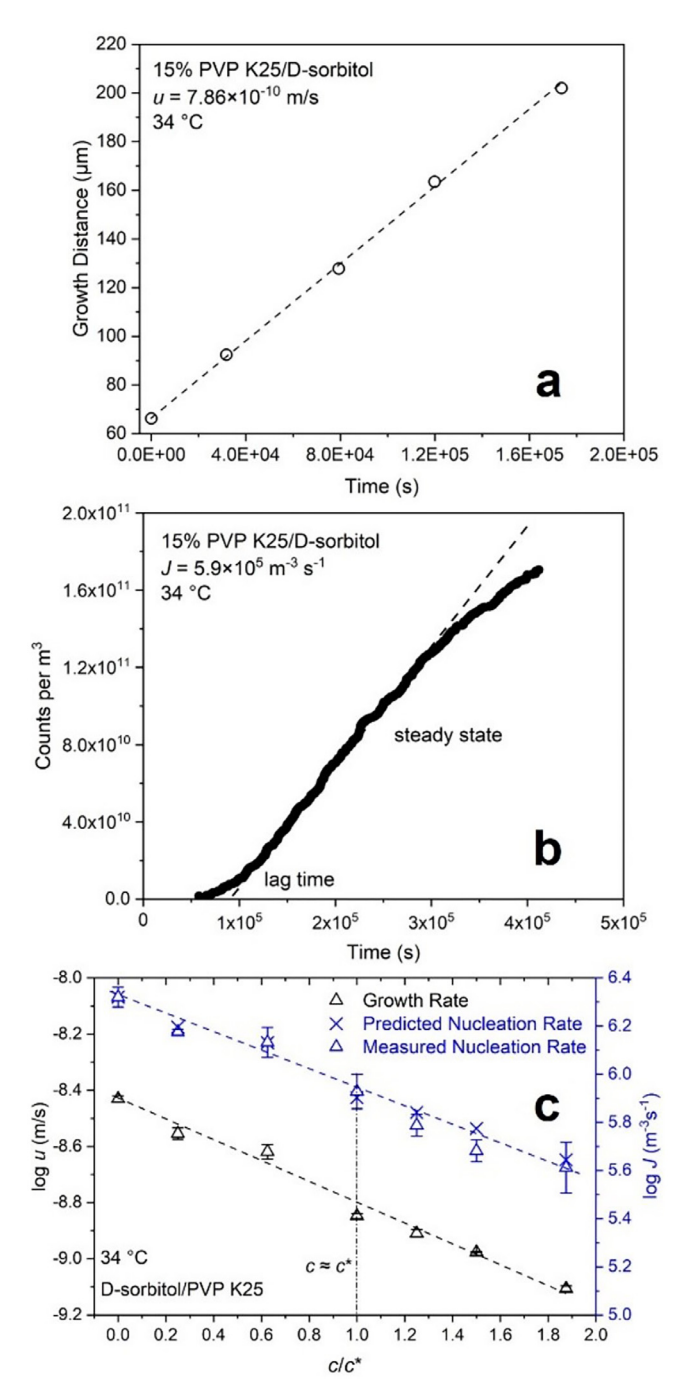


Fig. 5. (a) D-sorbitol crystal growth distance vs. time in the presence of 15 % PVP K25, the slope is the growth rate u. (b) One-stage method for measuring D-sorbitol nucleation rate in the presence of 15 % PVP K25 at 34 °C. The nucleation rate, J, is the slope of the nuclei density—time plot at steady state (dashed line). (c) Effect of rescaled PVP K25 concentration by e* on the steady state rates of crystal nucleation, J, and growth, u, in D-sorbitol at 34 °C.

Crystal Nucleation and Growth Rates of D-sorbitol/PVPs Below and Above c*

To affirm the exclusive role of the delay in first nucleation event on crystallization inhibition, the effects of polymer concentration on crystal nucleation rate, J, and growth rate, u, need to be accounted for. Fig. 5a shows typical data collected to measure crystal growth rate. The linear increase of D-sorbitol spherulite growth distance against time indicates a constant growth rate. Fig. 5b is a typical

nuclei density - time plot. The data show that after an induction period, a steady state is reached where the nuclei density (counts/ m³) increases linearly with time. The slope at steady state is the nucleation rate J (counts/m³/s). Fig. 5c shows the effect of PVP K25 concentration on the nucleation rate I and growth rate u in D-sorbitol at 34 °C. As c/c^* increases, J and u decrease at similar rates, following the relationship $\log(J/u) \approx 14.75 \text{ m}^{-4}$. This implies that both nucleation and growth share the same kinetic barrier and exhibit similar molecular motions (primarily rotational mobility altered by polymer segmental dynamics) in the supercooled state. 6,7,34-38 If so, the nucleation rate of binary systems can be predicted following $J = J_0(u/u_0)$, where J_0 and u_0 are nucleation and growth rates of the neat molecular liquid. The predicted nucleation rates at different c/c^* values, based on the experimentally measured growth rate in this study, are in excellent agreement with the experimentally measured nucleation rates (Fig. 5c). This phenomenon was first observed by Yao et al. in Dsorbitol/PVP K30 and D-arabitol/PVP K30 at lower temperatures. The smooth dependence of J and u on polymer concentration, both below and above c^* , for all four PVP molecular weight grades (Figs. 5c and S3-S5) also confirms that the significant suppression of crystallization above c^* is primarily correlated with the delay of the first nucleation event, but not steady state rate of crystal nucleation or growth.

Conclusions

We have measured the first nucleation time of glass forming molecular liquid D-sorbitol with four grades of PVP additives ($M_{\rm w}$ ranging from 4 K to 55 K) at various concentrations (\leq 30 %, below and above c^*). When PVP concentration c is less than the overlap concentration c^* , the first nucleation time is approximately identical to that of neat amorphous D-sorbitol. When PVP concentration exceeds c^* , the first nucleation event is significantly delayed but there is no abrupt change in the dependence of steady state rates of nucleation and growth on polymer concentration. These observations support the view that the effective inhibition against crystallization in multicomponent glasses above c^* is primarily correlated with the delay in the first nucleation event. Our findings are relevant for engineering multicomponent amorphous materials with sufficient stability against crystallization, especially in designing pharmaceutical amorphous formulations. Useful future directions of this work are (1) to examine the role of this mechanism (delay of the first nucleation event above c^*) on the surface nucleation of molecular glasses, given the strong surface nucleation effect in several molecular liquids, ³⁹⁻⁴¹ and (2) to investigate the impact of the presence of moisture on the crystal nucleation and growth kinetics, since moisture may enhance the molecular mobility of amorphous solids and hence accelerate nucleation kinetics.42

Declaration of competing interest

The authors declare that they have no known competing financial interests or personal relationships that could have appeared to influence the work reported in this paper.

Acknowledgments

S.S. thanks Chenguang Wang and Xin Yao for helpful discussions and David J.W. Grant & Marilyn J. Grant Fellowship for partial financial support. Synchrotron SAXS experiments were performed at the 5-ID-D beamline of the Advanced Photon Source (APS). This research used resources of the APS, a U.S. Department of Energy (DOE) Office of Science User Facility operated for the DOE Office of Science by Argonne National Laboratory under contract no. DE-ACO206CH11357. Part of this work was carried out in the Polymer

Characterization and Processing Facility, University of Minnesota (UMN), which has received capital equipment funding from the NSF through the UMN MRSEC program under award number DMR-2011401. Funding from Industrial Partners for Research in Interfacial and Materials Engineering (IPRIME) is also acknowledged. C.C.S. and R.A.S. thank the NSF for support through the Industry University Collaborative Research Center grant IIP-2137264, Center for Integrated Materials Science and Engineering for Pharmaceutical Products (CIM-SEPP).

Supplementary materials

Supplementary material associated with this article can be found in the online version at doi:10.1016/j.xphs.2024.02.011.

References

- Angell CA. Formation of glasses from liquids and biopolymers. Science. 1995;267 (5206):1924–1935.
- Berthier L, Biroli G, Bouchaud J-P, Cipelletti L, van Saarloos W. Dynamical Heterogeneities in Glasses, Colloids, and Granular Media. Oxford University Press; 2011.
- Yu L. Amorphous pharmaceutical solids: preparation, characterization and stabilization. Adv Drug Deliv Rev. 2001;48(1):27–42.
- Song S, Wang C, Wang S, Siegel RA, Sun CC. Efficient development of sorafenib tablets with improved oral bioavailability enabled by coprecipitated amorphous solid dispersion. *Int J Pharm.* 2021;610: 121216.
- Chiou WL, Riegelman S. Pharmaceutical applications of solid dispersion systems. J Pharm Sci. 1971;60(9):1281–1302.
- Huang C, Chen Z, Gui Y, Shi C, Zhang GGZ, Yu L. Crystal nucleation rates in glassforming molecular liquids: D-sorbitol, D-arabitol, D-xylitol, and glycerol. J Chem Phys. 2018;149(5): 054503.
- Yao X, Huang C, Benson EG, Shi C, Zhang GGZ, Yu L. Effect of polymers on crystallization in glass-forming molecular liquids: equal suppression of nucleation and growth and master curve for prediction. Cryst Growth Des. 2020;20(1):237–244.
- Newman A, Zografi G. Considerations in the development of physically stable high drug load API- polymer amorphous solid dispersions in the glassy state. J Pharm Sci. 2023;112(1):8–18.
- Goor OJGM, Hendrikse SIS, Dankers PYW, Meijer EW. From supramolecular polymers to multi-component biomaterials. Chem Soc Rev. 2017;46(21):6621–6637.
- Démuth B, Nagy ZK, Balogh A, et al. Downstream processing of polymer-based amorphous solid dispersions to generate tablet formulations. *Int J Pharm.* 2015;486(1):268–286.
- Song S, Wang C, Zhang B, Sun CC, Lodge TP, Siegel RA. A rheological approach for predicting physical stability of amorphous solid dispersions. *J Pharm Sci.* 2023;112 (1):204–212.
- Sahoo A, Suryanarayanan R, Siegel RA. Stabilization of amorphous drugs by polymers: the role of overlap concentration (c*). Mol Pharm. 2020;17(11):4401–4406.
- **13.** Sahoo A, Siegel RA. Drug-polymer miscibility and the overlap concentration (c^*) as measured by rheology: variation of polymer structure. *Pharm Res.* 2023;40 (9):2229–2237.
- 14. Huang C, Powell CT, Sun Y, Cai T, Yu L. Effect of low-concentration polymers on crystal growth in molecular glasses: a controlling role for polymer segmental mobility relative to host dynamics. J Phys Chem B. 2017;121(8):1963–1971.
- Yao X, Benson EG, Gui Y, Stelzer T, Zhang GGZ, Yu L. Surfactants accelerate crystallization of amorphous nifedipine by similar enhancement of nucleation and growth independent of hydrophilic–lipophilic balance. *Mol Pharm.* 2022;19 (7):2343–2350.
- Cai T, Zhu L, Yu L. Crystallization of organic glasses: effects of polymer additives on bulk and surface crystal growth in amorphous nifedipine. *Pharm Res.* 2011;28 (10):2458–2466.
- 17. Ishida H, Wu T, Yu L. Sudden rise of crystal growth rate of nifedipine near Tg without and with polyvinylpyrrolidone. *J Pharm Sci.* 2007;96(5):1131–1138.
- Deck L-T, Mazzotti M. Conceptual validation of stochastic and deterministic methods to estimate crystal nucleation rates. Cryst Growth Des. 2023;23(2):899–914.
- Evteev AV, Kosilov AT, Levchenko EV, Logachev OB. Kinetics of isothermal nucleation in a supercooled iron melt. *Phys Solid State*. 2006;48(5):815–820.
- Kirchner KA, Cassar DR, Zanotto ED, et al. Beyond the average: spatial and temporal fluctuations in oxide glass-forming systems. Chem Rev. 2023;123(4):1774–1840.
- Shah N, Iyer RM, Mair H-J, et al. Improved human bioavailability of vemurafenib, a
 practically insoluble drug, using an amorphous polymer-stabilized solid dispersion
 prepared by a solvent-controlled coprecipitation process. J Pharm Sci. 2013;102
 (31:967-981.
- Moseson DE, Parker AS, Beaudoin SP, Taylor LS. Amorphous solid dispersions containing residual crystallinity: influence of seed properties and polymer adsorption on dissolution performance. Eur J Pharm Sci. 2020;146: 105276.
- Yao X, Yu L, Zhang GGZ. Impact of crystal nuclei on dissolution of amorphous drugs. Mol Pharm. 2023;20(3):1796–1805.
- Silveira M, Jonas R. The biotechnological production of sorbitol. Appl Microbiol Biotechnol. 2002;59(4):400–408.

S. Song et al. / Journal of Pharmaceutical Sciences 00 (2024) 1-7

- 25. Doi M, Edwards SF. The Theory of Polymer Dynamics. Clarendon Press; 1986.
- 26. de Gennes PG. Scaling Concepts in Polymer Physics. Cornell University Press; 1979.
- 27. Yu L. Growth rings in d-sorbitol spherulites: connection to concomitant polymorphs and growth kinetics. Cryst Growth Des. 2003;3(6):967–971.
- Nezzal A, Aerts L, Verspaille M, Henderickx G, Redl A. Polymorphism of sorbitol. J Cryst Growth. 2009;311(15):3863–3870.
- **29**. Rukiah M, Lefebvre J, Hernandez O, van Beek W, Serpelloni M. Ab initio structure determination of the Γ form of D-sorbitol (D-glucitol) by powder synchrotron X-ray diffraction. *J Appl Cryst.* 2004;37(5):766–772.
- **30.** Schouten A, Kanters JA, Kroon J, Comini S, Looten P, Mathlouthi M. Conformational polymorphism of D-sorbitol (D-glucitol): the crystal and molecular structures of D-glucitol 2/3-hydrate and epsilond-glucitol. *Carbohydr Res.* 1998;312(3):131–137.
- 31. Lodge TP, Hiemenz PC. Polymer Chemistry. 3rd ed. CRC Press; 2020.
- 32. Zhang J, Liu Z, Wu H, Cai T. Effect of polymeric excipients on nucleation and crystal growth kinetics of amorphous fluconazole. *Biomater Sci.* 2021;9(12):4308–4316.
- Graessley WW. Polymeric Liquids & Networks: Structure and Properties. CRC Press; 2003.
- Morris RL, Amelar S, Lodge TP. Solvent friction in polymer solutions and its relation to the high frequency limiting viscosity. J Chem Phys. 1988;89(10):6523–6537.

- Fytas G, Rizos A, Floudas G, Lodge TP. Solvent mobility in polystyrene/aroclor solutions by depolarized Rayleigh scattering. J Chem Phys. 1990;93(7):5096–5104.
- Rizos A, Fytas G, Lodge TP, Ngai KL. Solvent rotational mobility in polystyrene/aroclor and polybutadiene/aroclor solutions. II. A photon correlation spectroscopic study. J Chem Phys. 1991;95(4):2980–2987.
- Schrag JL, Stokich TM, Strand DA, et al. Local modification of solvent dynamics by polymeric solutes. J Non-Cryst Solids. 1991;131-133:537-543.
- Lodge TP. Solvent dynamics, local friction, and the viscoelastic properties of polymer solutions. J Phys Chem. 1993;97(8):1480–1487.
- **39.** Yao X, Liu Q, Wang B, et al. Anisotropic molecular organization at a liquid/vapor interface promotes crystal nucleation with polymorph selection. *J Am Chem Soc.* 2022;144(26):11638–11645.
- Yao X, Borchardt KA, Gui Y, Guzei IA, Zhang GGZ, Yu L. Surface-enhanced crystal nucleation and polymorph selection in amorphous posaconazole. *J Chem Phys.* 2022;157(19): 194502.
- 41. Wu H, Yao X, Gui Y, Hao H, Yu L. Surface enhancement of crystal nucleation in amorphous acetaminophen. *Cryst Growth Des.* 2022;22(9):5598–5606.
- Li Y, Yu J, Tan X, Yu L. Surface mobility of amorphous indomethacin containing moisture and a surfactant: a concentration—temperature superposition principle. *Mol Pharm*. 2022;19(8):2962–2970.